

# Numerical Modelling of Microwave Devices

Eric A B Cole

Department of Applied Mathematical Studies,  
University of Leeds,  
Leeds LS2 9JT, UK

## Abstract

Various numerical routines are discussed and applied to the numerical simulation of a planar sub-micron gate length GaAs MESFET. The model contains energy transport and degenerate statistics. A generalisation of the Scharfetter-Gummel method is given which enables both the electron current density and energy flux to be easily coded. Degenerate statistics are included for the case in which the relaxation time is proportional to  $E^r$ . Steady state results are presented - these are arrived at both by iterating the transient solution and the direct method based on a modified Newton method.

## I Introduction

In this paper we look at the finite difference approach to the modelling of a two-dimensional MESFET. Other methods - the Finite Element method [1,2], the Boundary Element method and the Multigrid method [3] can be found elsewhere. To illustrate the general theory developed in Section IV, we will consider the simulation of a planar sub-micron gate length GaAs MESFET whose cross section in the x-y plane is shown in figure 1, with the ends of the source, gate and drain at  $x=s_0, s_1, g_0, g_1, d_0$  and  $d_1$ . The electron density  $n$ , electron temperature  $T_e$  and potential  $\psi$  will all be functions of  $x, y$  and time  $t$ . The equations are:

(i) the Poisson equation

$$\nabla^2 \psi = \frac{q}{\epsilon} (N_d - n) \quad (1)$$

where  $\epsilon$  is the product of the permittivity of the vacuum and the relative permittivity of the semiconductor. This equation is to be solved with the boundary conditions  $\psi=V_s$  on the source,  $\psi=V_d$  on the drain,  $\psi=V_g+\phi_b$  on the gate where  $\phi_b$  is the built-in potential, and  $\partial\psi/\partial n = 0$  at other parts of the

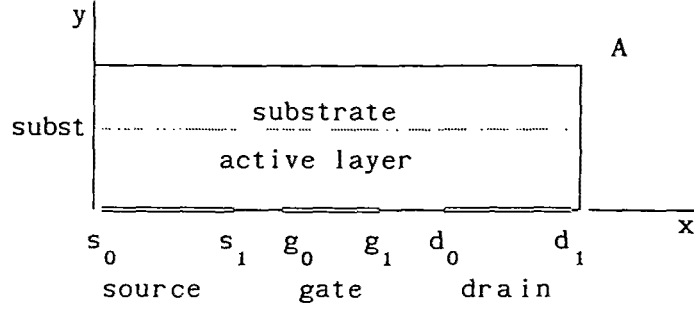


Fig. 1. Cross section of the MESFET.

boundary (In this paper,  $\underline{n}$  will represent the unit vector normal to the surface). The electric field is

$$\underline{E} = -\nabla\psi ; \quad (2)$$

(ii) the current continuity equation (neglecting recombination)

$$\frac{\partial n}{\partial t} = \frac{1}{q} \nabla \cdot \underline{J} \quad (3)$$

where the current density  $\underline{J}$  will have the form

$$\underline{J} = \alpha_c n(\nabla\psi) + \beta_c T_e (\nabla n) + \gamma_c n(\nabla T_e) \quad (4)$$

for certain coefficients  $\alpha_c$ ,  $\beta_c$  and  $\gamma_c$ . The boundary conditions taken here are  $n=2.5N_d$  on the source and drain,  $n=0$  on the gate, and  $\partial n/\partial \underline{n}=0$  elsewhere;

(iii) the energy transport equation

$$\frac{\partial W}{\partial t} = \underline{J} \cdot \underline{E} - \frac{(W-W_0)}{\tau(\xi)} - \nabla \cdot \underline{s} \quad (5)$$

where  $\xi$  is the (position and time-dependent) average electron energy,  $W=n\xi$ ,  $\tau(\xi)$  is the energy-dependent relaxation time, and  $\underline{s}$  is the energy flux

$$\underline{s} = \alpha_E W(\nabla\psi) + \beta_E T_e (\nabla W) + \gamma_E W(\nabla T_e) \quad (6)$$

for certain coefficients  $\alpha_E$ ,  $\beta_E$  and  $\gamma_E$ . The forms of all the coefficients will be discussed more fully in section V when particular statistics are introduced.

Having obtained a set of modelling equations, they should always be scaled to ensure a good numerical range for the variables [1,4].

## II Finite Differences

We will deal only with the special case of a non-uniform rectangular mesh. More general techniques including, for example, mesh refinement [1,5] and box generation [6] are described elsewhere. Consider the two-dimensional rectangular mesh shown in figure 2. Mesh points will be labelled  $0,1,2,\dots,M$  and  $0,1,2,\dots,N$  in the  $x$  and  $y$  directions respectively. The general mesh point will have coordinate  $(x_i, y_j)$ . The variable mesh spacings will be  $h_i = x_{i+1} - x_i$  ( $i=0,\dots,M-1$ ) and  $k_j = y_{j+1} - y_j$  ( $j=0,\dots,N-1$ ). The case of uniform mesh is given by  $h_i = h = \text{const.}$  and  $k_j = k = \text{const.}$  The value  $f(x_i, y_j)$  of any function  $f$  will be denoted shortly by  $f_{i,j}$ , while its value at the half-points  $(x_i + h_i/2, y_j)$ ,  $(x_i, y_j + k_j/2)$  and  $(x_i + h_i/2, y_j + k_j/2)$  will be denoted by  $f_{i+1/2,j}$ ,  $f_{i,j+1/2}$  and  $f_{i+1/2,j+1/2}$  respectively.

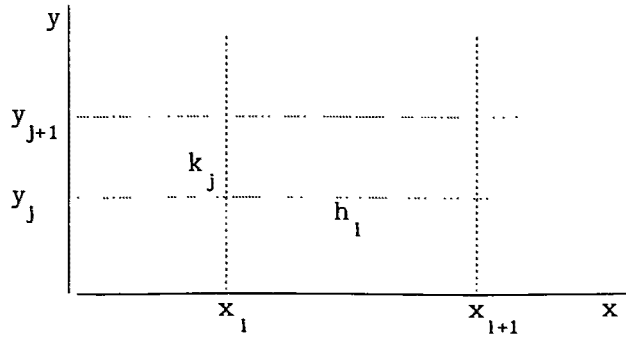


Fig. 2. The mesh.

Standard formulae exist for first and second order derivatives [7]. The important ones for this simulation are listed below (resorting to the one-dimensional case temporarily to ease the notation). The half-point formula for the first derivative of  $f$  is given by

$$f'_i = \frac{f_{i+1/2} - f_{i-1/2}}{(h_i + h_{i-1})/2} \quad (7)$$

where the next term  $-(h_i - h_{i-1})f''_i/4$  has been neglected. This is useful for evaluating divergences. The second order derivative at  $x_i$  can be written

$$f''_i = \frac{f'_{i+1/2} - f'_{i-1/2}}{(h_i + h_{i-1})/2} = \frac{(f_{i+1} - f_i)/h_i - (f_i - f_{i-1})/h_{i-1}}{(h_i + h_{i-1})/2}$$

and the neglected term here is  $(h_i - h_{i-1})f'''_i/3$ .

We often need an expression for the normal derivative at a boundary, in

which case it is very often zero. False nodes can be introduced outside the boundary but this increases storage requirements. Alternatively, this derivative may be expressed at  $x=0$  in terms of values at internal nodes by

$$f_0' = - \frac{h_1(h_1+2h_0)f_0 - (h_0+h_1)^2f_1 + h_0^2f_2}{h_0h_1(h_0+h_1)} \quad (8)$$

with a similar expression at  $x=x_M$ .

Returning to the case of functions of two variables, the Poisson equation  $\nabla^2\psi=g$  can be discretised in the form

$$\frac{\frac{\psi_{i+1,j} - \psi_{i,j}}{h_i} - \frac{\psi_{i,j} - \psi_{i-1,j}}{h_{i-1}}}{(h_i+h_{i-1})/2} + \frac{\frac{\psi_{i,j+1} - \psi_{i,j}}{k_j} - \frac{\psi_{i,j} - \psi_{i,j-1}}{k_{j-1}}}{(k_j+k_{j-1})/2} - g_{i,j} = 0. \quad (9)$$

In the case of uniform mesh this reduces to the standard 5-point formula

$$p^2\psi_{i-1,j} + p^2\psi_{i+1,j} + \psi_{i,j-1} + \psi_{i,j+1} - 2(1+p^2)\psi_{i,j} = p^2h^2g_{i,j} \quad (10)$$

where  $p=k/h$ . This equation has an error of order  $h^4$ , while the more accurate 9-point formula with error of order  $h^6$  is [8]

$$\begin{aligned} & (10p^2-2)(\psi_{i-1,j} + \psi_{i+1,j}) + (10-2p^2)(\psi_{i,j-1} + \psi_{i,j+1}) \\ & + (1+p^2)(\psi_{i-1,j-1} + \psi_{i+1,j-1} + \psi_{i-1,j+1} + \psi_{i+1,j+1}) - 20\psi_{i,j} \\ & = p^2h^2(g_{i-1,j} + g_{i+1,j} + g_{i,j-1} + g_{i,j+1} + 8g_{i,j}) \end{aligned} \quad (11)$$

### III Solution of Simultaneous Equations

The discretisation of the differential equations of the model generally gives rise to the problem of solving a set of  $M+1$  analytical equations of the form

$$f_i(X_0, X_1, \dots, X_M) = 0 \quad (i=0,1,\dots,M), \quad (12)$$

where the  $M+1$  values  $X_i$  will represent typical physical quantities at each point  $i$ . If there are  $\nu$  physical quantities described at each point, then the top index  $M$  is replaced by  $\nu(M+1)-1$ . The method of solution will depend on whether all the equations are linear or at least one equation is nonlinear.

## A. Linear Equations

When equations (12) are linear they take the form

$$\mathbf{A}\underline{X} = \underline{b} \quad (13)$$

where  $\mathbf{A}$  is an  $(M+1) \times (M+1)$  matrix and  $\underline{b}$  is an  $(M+1)$  component vector, both with elements which may depend on  $\underline{X}$ . These can be solved by direct methods or by indirect methods using iteration.

(a) Direct Methods. Very often the matrix is tridiagonal and a simple solution is available. Suppose that the equations have the form

$$\alpha_i X_{i-1} + \beta_i X_i + \gamma_i X_{i+1} = \delta_i \quad (i=0,1,\dots,M)$$

and the terms involving  $\alpha_0$  and  $\gamma_M$  do not appear. The standard method of eliminating down from the first equation and solving the resulting final two equations for  $X_{M-1}$  and  $X_M$  gives the solution

$$\begin{aligned} X_M &= \left[ (\beta'_{M-1})^{-1} \gamma_{M-1} - (\alpha_M)^{-1} \beta_M \right]^{-1} \left[ (\beta'_{M-1})^{-1} \delta'_{M-1} - (\alpha_M)^{-1} \delta_M \right] \\ X_i &= (\beta'_i)^{-1} \left[ \delta'_i - \gamma_i X_{i+1} \right] \quad (i=M-1, \dots, 0) \end{aligned} \quad (14)$$

where the  $\beta'_i$  and  $\delta'_i$  are generated by

$$\left. \begin{aligned} \beta'_0 &= \beta_0, & \delta'_0 &= \delta_0 \\ \beta'_1 &= \beta_1 - \alpha_1 (\beta'_{1-1})^{-1} \gamma_{1-1} \\ \delta'_1 &= \delta_1 - \alpha_1 (\beta'_{1-1})^{-1} \delta'_{1-1} \end{aligned} \right\} \quad (i=1, \dots, M-1).$$

Efficient coding of this routine is available [9,10]. We can usually get away without pivoting in this case because the simulation will probably not cause problems with the sizes of the elements of the tridiagonal system. In one-dimensional simulations which involve  $\nu$  physical variables at each node (for example,  $\nu=3$  when the variables are  $n$ ,  $p$  and  $\psi$ ), the equations at each node can be grouped so that equations (14) still hold. In that case, however, the  $X_i$ ,  $\delta_i$  and  $\delta'_i$  are  $\nu$ -component vectors and the quantities  $\alpha_i$ ,  $\beta_i$ ,  $\gamma_i$  and  $\beta'_i$  are  $\nu \times \nu$  matrices. The multiplications in equations (14) are in the correct order for matrix multiplication [11].

When  $\mathbf{A}$  is not simply tridiagonal, LU decomposition with partial pivoting

and scaling to control the growth of rounding errors may be used [10,12,13]. Rounding errors in direct methods can often be eliminated by solving the equation  $\underline{A}\underline{e} = \underline{b} - \underline{A}\underline{X}_c$  for the correction  $\underline{e}$  to the computed solution  $\underline{X}_c$ .

(b) Relaxation Methods. Consider the iterative process

$$\underline{X}^{k+1} = \underline{B}\underline{X}^k + \underline{c} \quad (15)$$

where the iteration matrix  $\underline{B}$  is an  $(M+1) \times (M+1)$  matrix with constant coefficients. If the solution converges to  $\underline{X}$  then equation (15) is equivalent to the equation  $(\underline{I} - \underline{B})\underline{X} = \underline{c}$ . Convergence may be slow if the spectral radius of  $\underline{B}$  is close to unity, so instead take a modified iteration process

$$\underline{X}^{k+1} = \underline{X}^k + w \left( \underline{c} - (\underline{I} - \underline{B})\underline{X}^k \right) = \underline{B}'\underline{X}^k + w\underline{c} \quad (16)$$

and adjust the value of the parameter  $w$  so that the spectral radius of  $\underline{B}'$  is as small as possible. This is the basis of the relaxation method.

In our original problem given by equation (13), we may write  $\underline{A} = \underline{L}_0 + \underline{D} + \underline{U}_0$  where  $\underline{D}$  is diagonal and  $\underline{L}_0$  and  $\underline{U}_0$  are lower and upper triangular with zeros on the diagonals. This decomposition suggests the Jacobi iteration

$$\underline{D}\underline{X}^{k+1} = \underline{b} - (\underline{L}_0 + \underline{U}_0)\underline{X}^k$$

with iteration matrix  $\underline{B} = -\underline{D}^{-1}(\underline{L}_0 + \underline{U}_0)$ , and the Gauss-Seidel iteration

$$(\underline{L}_0 + \underline{D})\underline{X}^{k+1} = -\underline{U}_0\underline{X}^k + \underline{b}$$

with iteration matrix  $\underline{B} = -(\underline{L}_0 + \underline{D})^{-1}\underline{U}_0$ . It can be shown [9,14,15] that the scheme (16) is convergent only for  $0 < w < 2$ . If  $0 < w < 1$  then we have Successive Under-Relaxation (SUR) while if  $1 < w < 2$  we have Successive Over-Relaxation (SOR). Further, the Jacobi spectral radius for equation (10) is

$$\rho_J = \frac{p^2 \cos \frac{\pi}{M+1} + \cos \frac{\pi}{N+1}}{1 + p^2}$$

with optimal choice  $w = \frac{2}{1 + (1 - \rho_J^2)^{1/2}}$ .

This is not the exact value for the equation (11) but it very often works well enough. See also [16]. The value of  $w$  may also be changed as the iteration progresses [17], for example, Chebyshev Acceleration.

## B. Non-linear Equations

The standard method here is the Newton-Raphson method. If  $\tilde{X}_c$  and  $\tilde{X} = \tilde{X}_c + \delta\tilde{X}$  are the computed and true solution, expansion of (12) to first order gives

$$J\delta\tilde{X} = -f(\tilde{X}_c) \quad \text{where} \quad J_{ij} \equiv \left. \frac{\partial f_i}{\partial X_j} \right|_c$$

is the Jacobian. This is a set of linear equations which can be solved (among other methods) using the iteration scheme

$$J^k \delta\tilde{X}^k = -f(\tilde{X}^k), \quad \tilde{X}^{k+1} = \tilde{X}^k + \alpha \delta\tilde{X}^k$$

where  $\alpha$  is taken such that  $0 < \alpha \leq 1$  to avoid overshoot. It is usually necessary to take  $\alpha$  small in the early stages of the iteration and then to steadily increase it as the iteration progresses.

An alternative Newton method has been found to make iterations go more smoothly. Instead of solving for  $\delta\tilde{X}^k$  we solve directly for  $\tilde{X}^{k+1}$  :

$$J\tilde{X}^{k+1} = J(\tilde{X}^k + \alpha\delta\tilde{X}^k) = J\tilde{X}^k - \alpha f^k. \quad (17)$$

The advantages here are that we can usually take larger values of  $\alpha$  and that fewer initial guesses need to be made. When  $J_{11} \neq 0$  ( $1=0, \dots, M$ ) then (17) becomes

$$X_1^{k+1} = J_{11}^{-1} \left( (-\alpha f_1 + JX^k)_1 - \sum_{j \neq 1}^M J_{1j} X_j^{k+1} \right)$$

with corresponding iteration process

$$X_1^{k+1} = (1-w)X_1^{k+1} + wJ_{11}^{-1} \left( (-\alpha f_1 + JX^k)_1 - \sum_{j \neq 1}^M J_{1j} X_j^{k+1} \right) \quad (18)$$

where  $f_1 \equiv f(\tilde{X}^k)$  and  $J \equiv J(\tilde{X}^k)$ . If  $\tilde{X}$  represents a natural grouping of  $\nu$  quantities at each point (that is,  $X_1$  is a  $\nu$ -component vector) then equation (18) still holds with  $J_{11}$  being a  $\nu \times \nu$  nonsingular matrix, and  $w$  as a  $\nu \times \nu$  diagonal matrix with separate relaxation factors down the diagonal.

Evaluation of the Jacobian can be the most time-consuming part of the operation. It is possible to differentiate the functions  $f_1$  numerically using

$$\frac{\partial f_1}{\partial X_j} \approx \frac{f(X_0, \dots, X_j + \Delta X_j, \dots, X_M) - f(X_0, \dots, X_j, \dots, X_M)}{\Delta X_j}$$

where the  $\Delta X_j$  are suitable increments. If the  $\Delta X_j$  are too small then roundoff

errors can swamp the calculation, while convergence will be linear if they are too large [18]. Methods could be used in which, say, standard functions are differentiated explicitly while, for example, mobility curves fed in from other simulations could be differentiated numerically. Also using Broyden's rank one correction it is not necessary to evaluate  $\mathbf{J}$  at each iteration [19].

#### IV Discretising the Current Continuity and Energy Equations

An explicit time discretisation of the current continuity equation will only work if the timestep  $\Delta t$  is excessively small [20], while a fully implicit Crank-Nicholson scheme [12] is difficult to solve. The linearised semi-implicit scheme [21] is more satisfactory unless  $\Delta t$  is taken too large. This limitation can be avoided if we use, in the case of constant  $T_e$ , the Scharfetter-Gummel method in which we take an exponential variation in the carrier deviations between nodes [22,23].

The following is a generalisation of the Scharfetter-Gummel method when  $T_e$  is not constant throughout the device. Equations (4) and (6) can be written in general form

$$\underline{V} = \alpha(\nabla\psi)\theta + \beta T_e(\nabla\theta) + \gamma\theta(\nabla T_e) \quad (19)$$

where ( $\underline{V} \equiv \underline{J}$ ,  $\theta \equiv n$ ) for the current density and ( $\underline{V} \equiv \underline{S}$ ,  $\theta \equiv W$ ) for the energy flux. For numerical purposes only we now make the assumptions that, in the interval  $(i,j) \rightarrow (i+1,j)$ , the quantities  $\nabla\psi$ ,  $\nabla T_e$ ,  $\beta$ ,  $\alpha/\beta$  and  $\gamma/\beta$  are constants. The x-component of equation (19) becomes

$$\frac{\partial \theta}{\partial x} + \left[ \frac{\gamma}{\beta} \frac{1}{T_e} \frac{\partial T_e}{\partial x} + \frac{\alpha}{\beta} \frac{1}{T_e} \frac{\partial \psi}{\partial x} \right] \theta = \frac{1}{T_e} \left( \frac{V_x}{\beta} \right)_{i+1/2,j}$$

which has integrating factor

$$\exp \left[ \int \left( \frac{\gamma}{\beta} \frac{1}{T_e} \frac{\partial T_e}{\partial x} + \frac{\alpha}{\beta} \frac{1}{T_e} \frac{\partial \psi}{\partial x} \right) dx \right] = T_e^r \quad (20)$$

where  $r \equiv \frac{\gamma}{\beta} + \frac{\alpha}{\beta} \frac{\partial \psi}{\partial x} \left( \frac{\partial T_e}{\partial x} \right)^{-1}$  and quantities  $\gamma/\beta$  etc are evaluated at  $(i+1/2,j)$ . The resulting equation is

$$\frac{\partial}{\partial x} (\theta T_e^r) = T_e^{r-1} \left( \frac{V_x}{\beta} \right)_{i+1/2,j}$$

which can be integrated between  $x=x_i$  and  $x=x_{i+1}$  and re-arranged to give

$$\begin{aligned}
(V_{x,1+1/2,J}) &= \frac{\beta_{1+1/2,J}}{h_1} \left[ C_{\gamma/\beta} \left( -\frac{\alpha}{\beta} (\psi_{1+1,J} - \psi_{1,J}), T_{1+1,J}, T_{1,J} \right) \theta_{1+1,J} \right. \\
&\quad \left. - C_{\gamma/\beta} \left( \frac{\alpha}{\beta} (\psi_{1+1,J} - \psi_{1,J}), T_{1,J}, T_{1+1,J} \right) \theta_{1,J} \right] \quad (21)
\end{aligned}$$

with a similar expression for  $(V_{y,1,J+1/2})$ . Here,  $C$  is the function defined by

$$C_a(x,y,z) \equiv p(y,z) B\left(\frac{x-a(y-z)}{p(y,z)}\right) \quad (y \neq z) \quad (22)$$

where  $p(y,z) \equiv \frac{(z-y)}{\ln(z/y)}$  and  $B(t) \equiv \frac{t}{e^t - 1}$  is the Bernoulli function.

One important property of this  $C$ -function, namely

$$\lim_{T \rightarrow T_0} C_a(x, T_0, T) = T_0 B(x/T_0)$$

is useful for applying to models in which the electron temperature is a constant  $T_0$ , and the original Scharfetter-Gummel expression is then obtained.

It is necessary to avoid overflows and underflows when evaluating the  $C$ -functions. The usual method [1] is to make a piecewise machine-dependent approximation for  $B(t)$ . The derivative of the Bernoulli function can be approximated by

$$B'(t) = \begin{cases} (t-2)/4 & \text{for } t_2 \leq t \leq t_3 \\ \frac{B(t)}{t} (1-B(t)-t) & \text{otherwise.} \end{cases}$$

## V Evaluation of the Coefficients

The Fermi integral  $F_r(\eta)$  is defined as

$$F_r(\eta) \equiv \Gamma(r+1)^{-1} \int_0^{\infty} y^r (1 + e^{y-x})^{-1} dy \quad \text{where} \quad \Gamma(r+1) \equiv \int_0^{\infty} y^r e^{-y} dy$$

This function has been extensively approximated and tabulated [24]. Write  $k_B$  as Boltzmann's constant,  $h_p$  as Planck's constant,  $\mu$  as the mobility,  $m_e$  as the effective electron mass,  $\eta \equiv (E_F - E_c)/(k_B T_e)$ , and take the energy dependence of the relaxation time as  $\tau \propto (E - E_c)^r$ . The first few moments of the Boltzmann transport equation then give [25,26]

$$n = AT_e^{3/2} F_{1/2}(\eta) \quad \text{where} \quad A \equiv 2(2\pi k_B m_e)^{3/2} / h_p^3 ,$$

$$W = \frac{3}{2} k_B T_e n F_{3/2}(\eta) / F_{1/2}(\eta) ,$$

$$\underline{J} = \mu n (-q \nabla \psi + k_B T_e \nabla \eta) + I_2 (\nabla T_e) / T_e ,$$

$$q \underline{s} = -I_2 (-q \nabla \psi + k_B T_e \nabla \eta) - I_3 (\nabla T_e) / T_e$$

where

$$I_2 \equiv \mu n (r + \frac{5}{2}) k_B T_e F_{r+3/2} / F_{r+1/2}$$

$$I_3 \equiv I_2 (r + \frac{7}{2}) k_B T_e F_{r+5/2} / F_{r+3/2} .$$

After extensive manipulation and using the constant effective mass approximation, it is found that  $\underline{J}$  and  $\underline{s}$  have the forms (4) and (6) where

$$\alpha_c = -q\mu$$

$$\beta_c = k_B \mu F_{1/2} / F_{-1/2}$$

$$\gamma_c = k_B \mu \left( (r + \frac{5}{2}) F_{r+3/2} / F_{r+1/2} - \frac{3}{2} F_{1/2} / F_{-1/2} \right)$$

$$\alpha_E = \frac{2}{3} \mu (r + \frac{5}{2}) F_{r+3/2} F_{1/2} / (F_{r+1/2} F_{3/2})$$

$$\beta_E = -\frac{2}{3} k_B \mu (r + \frac{5}{2}) F_{r+3/2} / (q F_{r+1/2})$$

$$\gamma_E = \frac{2}{3} k_B \mu (r + \frac{5}{2}) \left( \frac{5}{2} F_{r+3/2} / F_{r+1/2} - (r + \frac{7}{2}) F_{r+5/2} F_{1/2} / (F_{r+1/2} F_{3/2}) \right) / q$$

and  $F_i \equiv F_i(\eta)$  throughout.

At certain stages of the numerical implementation it is necessary to find  $\eta$  and  $T_e$  at each point given the values of  $n$  and  $W$ . From the above, it may be shown that

$$F_{1/2}(\eta)^5 / F_{3/2}(\eta)^3 = 54 h_p^6 (8\pi m_e)^{-3} n^5 / W^3 \quad (23)$$

and this may be inverted to give  $\eta$  and hence  $T_e$  from

$$T_e = \frac{2}{3} W F_{1/2}(\eta) / [k_B n F_{3/2}(\eta)] .$$

Conversely, to find  $\eta$  and  $W$  given  $n$  and  $T_e$ ,  $\eta$  may be calculated at each point by inverting the equation

$$F_{1/2}(\eta) = n/(AT_e^{3/2}) \quad (24)$$

and calculating W from

$$W = \frac{3}{2} k_B T_e n F_{3/2}(\eta) / F_{1/2}(\eta) .$$

Both these inversions must be done at each grid point. Once the functions  $F_{1/2}$  and  $F_{3/2}$  have been programmed, inversion is straightforward since the left hand sides of equations (23) and (24) are strictly increasing functions of  $\eta$ .

## VI Implementation for the MESFET

We now apply the preceding results to the simulation of the MESFET model outlined in section I. Referring to figure 1, the dimensions taken were  $s_0=0.0\mu\text{m}$ ,  $s_1=0.2\mu\text{m}$ ,  $g_0=0.6\mu\text{m}$ ,  $g_1=1.1\mu\text{m}$ ,  $d_0=1.6\mu\text{m}$  and  $d_1=1.8\mu\text{m}$ . The total thickness including substrate was  $0.45\mu\text{m}$ . An abrupt junction at  $y=0.35\mu\text{m}$  was taken with

$$N_d = \begin{cases} 10^{23} \text{ m}^{-3} & \text{for } 0\mu\text{m} \leq y \leq 0.35\mu\text{m} \\ 10^{19} \text{ m}^{-3} & 0.35\mu\text{m} < y \leq 0.45\mu\text{m}. \end{cases}$$

Monte Carlo simulations and experimental data on the steady state transport characteristics provide curves of  $\xi$  and  $\tau$  in terms of the static electric field  $E_{ss}$  which is used as an intermediate parameter. This enables  $\tau$  to be found in terms of  $\xi$ . The mobility is given by

$$\mu = \frac{300\mu_0}{T_0} \left[ \frac{1 + \frac{8.5 \times 10^4 E^3}{\mu_0 (1 - 5.3 \times 10^{-4} T_0) E_0^4}}{1 + (E/E_0)^4} \right] \quad \text{where} \quad \mu_0 = \frac{0.8}{1 + (N_d/10^{23})^{1/2}}$$

and  $E=4 \times 10^5 \text{ Vm}^{-1}$ . All boundary conditions  $\partial/\partial \underline{n}=0$  were implemented using equation (8) and its equivalents with all derivatives zero. The quantities  $\underline{j}$  and  $\underline{s}$  were coded at the half points using appropriate values in expression (21). Three solutions were performed: the transient solution, the steady state reached by iterating the transient solution, and the direct solution of the steady state.

(a) The transient solution. A timestep  $\Delta t=10^{-14} \text{ s}$  was used. The Poisson equation (11) was used to extract an expression  $A_{1,j}$  for  $\psi_{1,j}$  in terms of the other quantities, and was solved by iterating the equation

$$\psi_{1,j} = (1-w_{\text{psi}})\psi_{1,j} + w_{\text{psi}} A_{1,j} .$$

The current continuity and energy equations (3) and (5) were similarly solved by coding the C functions with the appropriate quantities  $\alpha_c, \dots, \gamma_e$ . It was found that the separate relaxation factors  $w_{\text{psi}}=1.4$ ,  $w_n=0.8$  and  $w_T=0.5$  gave the fastest iteration. At each timestep, the three equations were iterated separately inside an overall iteration. A mixture of convergence tests was used. In the case of the  $\psi$  iteration, we required convergence at each point, that is, we required that  $|\psi_{1,j} - \psi_{1,j}^1|$  had to be less than some prescribed value at every point, where  $\psi^1$  was the value at the previous iteration. The same test was applied to the electron temperature  $T_e$ . In the case of the  $n_{1,j}$  we applied a weaker test by requiring that only the average relative difference  $\sum |n_{1,j} - n_{1,j}^1| / n_{1,j}$  be smaller than some prescribed value. It was found that this average condition gave a smoother time plot of the total current

$$J_{\text{tot}} = \int_0^{0.45} \left( J_x + \epsilon \partial E_x / \partial t \right) dy .$$

(b) Iteration to the steady state. The method of (a) was used but with no iteration of the equations at each timestep. A total of 2000 timesteps was used, giving a device time of 20ps. Results for  $\psi$ ,  $n$  and  $T_e$  are shown in figure 3 (viewed from corner A in figure 1) for the case  $r=-1$ .

(c) Direct method. A natural grouping  $\tilde{X}_{1,j} = (\psi_{1,j}, n_{1,j}, T_{e1,j})^T$  exists at each gridpoint (i,j). Put all  $\partial/\partial t$  terms zero in equations (1), (3) and (5) and write the equations generally as  $G_1=0$ ,  $G_2=0$  and  $G_3=0$ . The Newton method applied at each point gives

$$A \delta \tilde{X}_{1-1,j} + B \delta \tilde{X}_{1+1,j} + C \delta \tilde{X}_{1,j} + D \delta \tilde{X}_{1,j-1} + E \delta \tilde{X}_{1,j+1} = -\tilde{G}$$

where  $A_{m1} \equiv \partial G_m / \partial \psi_{1-1,j}$  etc are  $3 \times 3$  matrices. Writing  $\tilde{y}_{1,j} \equiv \tilde{X}_{1,j} + \alpha \delta \tilde{X}_{1,j}$ , the modified Newton method (18) becomes

$$\tilde{y}_{1,j}^{k+1} = (I-w) \tilde{y}_{1,j}^{k+1} + w C^{-1} \left( -\alpha \tilde{G} + A \tilde{X}_{1-1,j}^k + B \tilde{X}_{1+1,j}^k + C \tilde{X}_{1,j}^k + D \tilde{X}_{1,j-1}^k + E \tilde{X}_{1,j+1}^k \right. \\ \left. - A \tilde{y}_{1-1,j}^{k+1} - B \tilde{y}_{1+1,j}^{k+1} - D \tilde{y}_{1,j-1}^{k+1} - E \tilde{y}_{1,j+1}^{k+1} \right)$$

where  $w$  is the diagonal matrix with nonzero elements  $w_{\text{psi}}$ ,  $w_n$  and  $w_T$ . This routine is fragile in the early stages, and for the first few Newton iterations it is necessary to take  $\alpha$  very small (typically 0.01),  $n_{1,j}$  to be kept positive and  $T_{e1,j}$  to be not less than  $T_0$ .

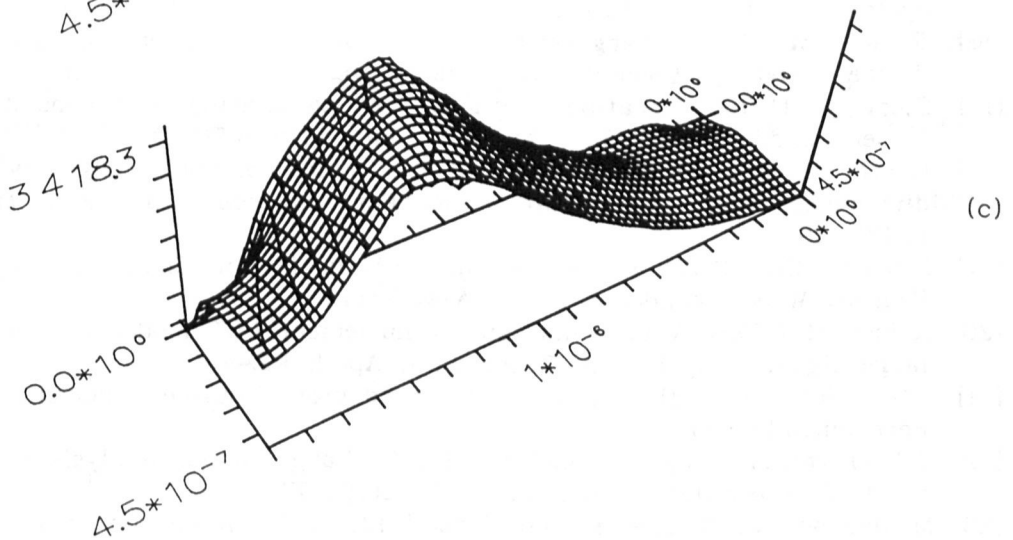
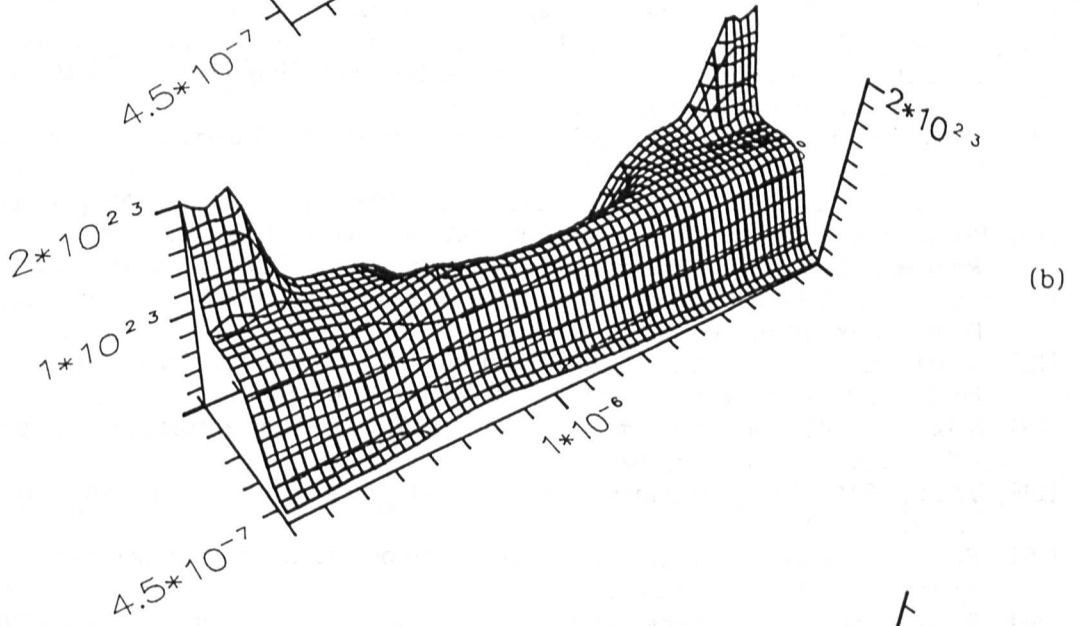
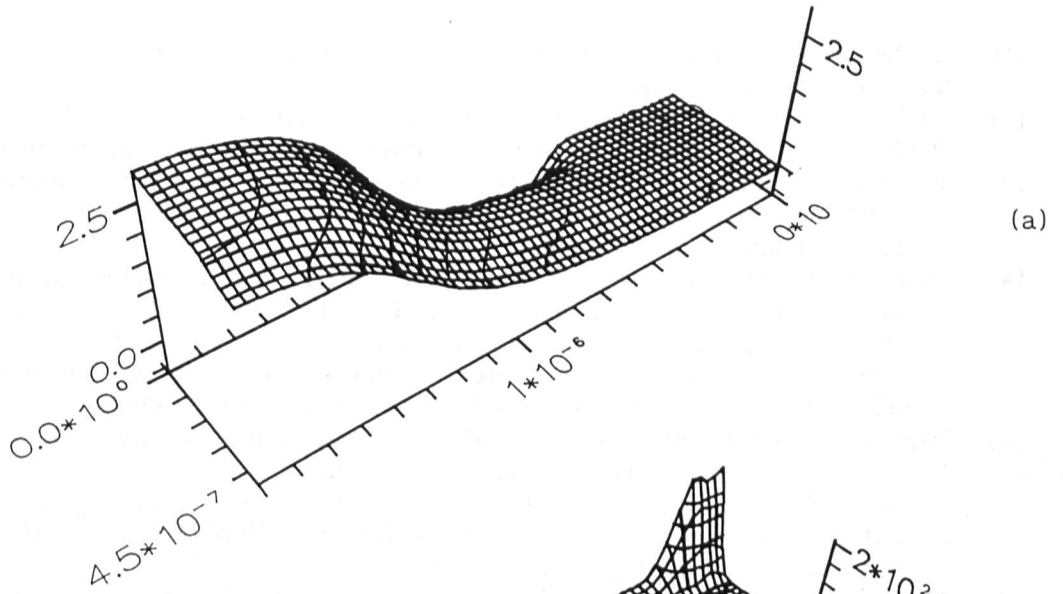


Fig.3. Steady-state results for (a) potential  $\psi$ , (b) electron density  $n$ , and (c) electron temperature  $T_e$ .

## References

- [1] Selberherr S (1984) Analysis and simulation of semiconductor devices. Springer-Verlag, Vienna, New York
- [2] Mobbs SD (1989) Numerical techniques - finite element. Semiconductor Device Modelling (Snowden CM ed., Springer-Verlag, London, Berlin):49-59
- [3] Ingham DB (1989) Numerical techniques - finite difference and boundary element method. Semiconductor Device Modelling (Snowden CM ed, Springer-Verlag, London, Berlin):34-48
- [4] Xue H, Howes MJ and Snowden CM (1991) The modified semiconductor equations and associated algorithms for physical simulation. Int J Num Modelling: Electronic Networks, Devices and Fields 4:107-122
- [5] De Mari A (1968) An accurate numerical steady-state one-dimensional solution of the p-n junction. Solid State Electronics 11:33-58
- [6] Barton T (1989) Computer simulations. Semiconductor Device Modelling (Snowden CM ed, Springer-Verlag, London, Berlin):227-247
- [7] Cole EAB (1993) Numerical methods and their application to device modelling. Compound Semiconductor Device Modelling (Snowden CM and Miles RE eds, Springer-Verlag, London, Berlin):1-25
- [8] Scraton RE (1987) Further numerical methods. Edward Arnold, London, Baltimore
- [9] Varga RS (1962) Matrix iterative algebra. Prentice Hall Inc, New Jersey
- [10] Press WH, Flannery BP, Teukolsky SA and Vetterling WT (1986) Numerical Recipes. Cambridge University Press, Cambridge, London, New York
- [11] Kurata M (1982) Numerical analysis for semiconductor devices. Lexington Books, Lexington, Toronto
- [12] Smith GD (1985) Numerical solution of partial differential equations: finite difference methods. Clarendon Press, Oxford
- [13] Wilkinson JH and Reinsch C (1971) Handbook for automatic computation, vol 2. Springer-Verlag, Berlin
- [14] Young DM (1971) Iterative solution of large linear systems. Academic Press, New York
- [15] Stoer J and Bulirsch R (1980) Introduction to numerical analysis. Springer-Verlag, New York
- [16] Reiser M (1972) Large-scale numerical simulation in semiconductor device modelling. Computer Methods in App Mech and Eng 1:17-38
- [17] Stern F (1970) Iteration methods for calculating self-consistent fields in semiconductor inversion layers. J Comp Phys 6:56-67
- [18] Curtis A and Reid JK (1974) The choice of step-length when using differences to approximate Jacobian matrices. J Inst Math Appl 13:121-126
- [19] Broyden CG (1972) in Numerical methods for unconstrained optimisation (Murray W ed., Academic Press, New York)
- [20] Reiser M (1972) A two-dimensional numerical FET model for dc- ac- and large signal analysis. IBM Research J, April, RZ499
- [21] Snowden CM(ed) (1988) Semiconductor device modelling. Peter Peregrinus, London
- [22] Scharfetter DL and Gummel HK (1969) Large signal analysis of a silicon Read diode oscillator. IEEE Trans ED-16:64-77
- [23] McAndrew CC, Singhal K and Heasell EL (1985) A consistent nonisothermal extension of the Scharfetter-Gummel stable difference approximation. IEEE ED Lett EDL6:446-447
- [24] Blakemore JS (1982) Approximations for Fermi-Dirac integrals. Solid State Electronics 25:1067-1076
- [25] de Graaff HC and Klaassen FM (1990) Compact transistor modelling for circuit design. Springer-Verlag, Wien, New York
- [26] Stratton R (1972) Semiconductor current-flow. IEEE Trans ED-19:1288-1292